

Brief Report

Marble Chromatic Alteration Study Using Non-Invasive Analytical Techniques and Evaluation of the Most Suitable Cleaning Treatment: The Case of a Bust Representing Queen Margherita di Savoia at the U.S. Embassy in Rome

Andrea Macchia ^{1,2}, Eleonora Cerafogli ^{3,*}, Laura Rivaroli ⁴, Irene Angela Colasanti ², H el ene Aureli ², Chiara Biribicchi ⁵ and Valeria Brunori ⁶

¹ Department of Biology, Ecology and Earth Sciences (DiBEST), University of Calabria, Via Pietro Bucci, Arcavacata, 87036 Rende, Italy

² YOCOCU (Youth in Conservation of Cultural Heritage), Via T. Tasso 108, 00185 Rome, Italy

³ Department of Environmental Biology, University of Rome La Sapienza, P.le Aldo Moro 5, 00185 Rome, Italy

⁴ Department of Cultural Heritage, University of Bologna, Via Zamboni 33, 40126 Bologna, Italy

⁵ Department of Earth Sciences, University of Rome La Sapienza, P.le Aldo Moro 5, 00185 Rome, Italy

⁶ OBO/OPS/Office of Cultural Heritage, U.S. Embassy Rome, Via Vittorio Veneto 121, 00187 Rome, Italy

* Correspondence: eleonora.cerafogli@uniroma1.it



Citation: Macchia, A.; Cerafogli, E.; Rivaroli, L.; Colasanti, I.A.; Aureli, H.; Biribicchi, C.; Brunori, V. Marble Chromatic Alteration Study Using Non-Invasive Analytical Techniques and Evaluation of the Most Suitable Cleaning Treatment: The Case of a Bust Representing Queen Margherita di Savoia at the U.S. Embassy in Rome. *Analytica* **2022**, *3*, 406–429. <https://doi.org/10.3390/analytica3040028>

Academic Editor: Marcello Locatelli

Received: 29 August 2022

Accepted: 28 October 2022

Published: 3 November 2022

Publisher's Note: MDPI stays neutral with regard to jurisdictional claims in published maps and institutional affiliations.



Copyright:   2022 by the authors. Licensee MDPI, Basel, Switzerland. This article is an open access article distributed under the terms and conditions of the Creative Commons Attribution (CC BY) license (<https://creativecommons.org/licenses/by/4.0/>).

Abstract: In spite of the application of different cleaning procedures, the marble used for the portrait bust of Queen Margherita di Savoia continued to show permanent discoloration, consisting of an unevenly distributed grayish alteration, mainly on the front part. In this work, a multi-analytical, non-invasive approach was proposed using spectrophotometry, reflectance spectroscopy and multispectral imaging. The initial assumption, suggesting the presence of altered protective materials based on organic products (such as waxes or oils,) applied in the past according to traditional practices, was excluded, revealing instead the presence of deposits of particulate matter, which penetrated inside the crystalline structure of the marble, leading to a variation in its shade. Cleaning tests were also carried out to define the best product, using sustainable chemicals such as Polar Varnish Rescue[ ], alkoxyde surfactant, disodium EDTA, GLDA and Politect[ ] Base in order to identify the best methodology and materials for sustainable cleaning, respecting the integrity of the original matter. Politect[ ] Base demonstrated better action in comparison to the other products tested, and similar results were obtained with GLDA, which could be applied in areas where the Politect[ ] is less efficient (e.g., lace).

Keywords: diagnostics; stone; non-invasive; multispectral imaging; colorimetry; reflectance spectroscopy; green chemistry; U.S. Embassy

1. Introduction

Stone materials were largely employed for artworks and architectures. Although stone properties make them extremely durable, stone is still subject to weathering phenomena in certain conditions. The most common weathering effect is marble discoloration, which can be attributed to many causes:

- Black crusts formed by the action of acid rains that can dissolve calcium carbonate (the main component of marble) and create gypsum depositions able to absorb air particles, causing a blackening of the surface and the corrosion of the marble [1–4];
- Dirt, dust and air particulate depositions can penetrate inside marble porosity [5,6];
- The presence of metals in contact with the stone and water can produce leakages and stains of the oxidized metal on the surface [7–10];
- Black fungi, lichens and bacteria not only create a colored patina on the surface, but can also lead to the formation of colored calcium oxalates [11–14];
- Aged protective products from previous restorations [15,16];

Analysis and characterization of discolorations and crusts on marble are of primary concern for restorers, as they choose the appropriate conservation treatment. As testified by many authors [17], inappropriate cleaning operations could even damage the stone, causing loss of the original surface, staining, soluble salts depositions and superficial roughening, making it a lot more vulnerable to biological attack and pollutants.

Marble cleaning methodologies can be divided into mechanical, chemical, physical and biological types:

Mechanical methods involve brushing, rubbing and blasting. Abrasive blasting (wet or dry) is conventionally used to remove solid superficial deposits of dirt and dust or black crusts, commonly by using sand ejected at high pressure (sandblasting) [18]. The abrasive power should be carefully selected based on the coherence of the deposition and the conservation status of the stone, taking into consideration the hardness of the particles, grain size, grain shape, nozzle size and pressure. This type of cleaning is cheap and very effective, but it lacks control by the operator, which can result in damage to the stone surface [19]. A step forward for this technique is the use of very fine particles of silica and glass beads (microblasting), able to achieve a milder action and a more adequate level of control by the operator [19];

Chemical cleaning involves the use of acids and alkali that could be dangerous, as calcium carbonate can be dissolved by strong acids, like hydrochloric acid, and strong alkali can cause saponification of fatty acid stains on stone surfaces; moreover, when used as a second cleaning phase after an acid, it can cause the formation of soluble salts [19]. Organic solvents are used to remove oily stains, waxes and bituminous compounds, and are also commonly used as biocides for the removal of biological patinas (fungi, bacteria, algae, lichens). A drawback in the use of these substances is that they can penetrate inside the porosities and cause further deterioration. To avoid this, absorbent powders, clays, poultices and gels are used to retain solvents and guarantee a superficial action [20]. Commonly used solvents are also noticeably dangerous for the health and environment [21];

Laser cleaning [22] is the only available physical technique. It can efficiently remove stains and crusts, except for in some cases. However, possible alterations can be induced by this technique when the working regime is not properly chosen. This is why laser cleaning requires thorough testing prior to operation [23];

Biocleaning is a more recent approach born of the necessity to search for a safer and more selective methodology; this technique uses specific strains of bacteria to remove patinas, salts and crusts [24]. Although it is an excellent sustainable and selective method and showed encouraging results, technological transfer on a larger scale and availability of products that are ready to use are problems that still need to be solved [24].

The marble bust representing Margherita di Savoia by Odoardo Fantacchiotti (1811–1877) was completed in 1869, as stated on the inscription visible on the reverse of the sculpture: “OD°: FANTACCHIOTTI/SCOLPIVA IN FIRENZE/L'ANNO 1869” (in total, the bust measures 47 cm wide, 28 cm deep and 85 cm high; the base alone measures 22 cm wide, 22 cm deep and 14.5 cm high). The portrait represents young Princess Margherita in a pensive mood; the head leans slightly to the left, the look is melancholic and the hair is tied up in a braid fastened to the rear of the head in a circle. A few locks of hair protrude onto the forehead. The neck and shoulders are bare, and the rich ball gown shows a generous neckline and consists of a corset trimmed with a pleated edge and secured with ribbon tied in a small bow; an intricately ornate lace draped around the figure's shoulders covers the corset and is held at the center by a pin in the shape of a daisy, referring to the subject's name. The quadrangular pedestal with concave sides is finished at the upper end with a quarter-round echinus decorated by the classical eggs-and-darts motif, while the torus at its base is articulated in a continuing cane bundle held tight by a twisted flat band. The Savoia family crest with the single cross of the Piedmont branch occupies the front of the base, topped with the royal crown flanked by fluttering ribbons. From 1901 until shortly before her death in 1926, Margherita lived as the Queen Mother in the palace that presently houses the U.S. Embassy's chancery in Rome [25–29]. The property was purchased by

her son, King Vittorio Emanuele III, on 24 December 1900, after the assassination of King Umberto I and his accession to the throne [29]; the palace was her residence in the new capital of Italy during a period of deep changes that led the country through two world wars and the fascist regime.

Since the purchase of Palazzo Margherita by the U.S. Government in 1946 (sales purchase contract 1946 in Archivio Centrale dello Stato-PCM, 1944–1947, 71488/7.2-‘Acquisto dello stabile Palazzo Margherita’), the marble portrait of the Queen became part of the U.S. Embassy’s permanent art collection and as such is included in the cultural patrimony’s conservation and maintenance program, conducted by the Cultural Heritage Office since 1998. Exhibited in the grand staircase of the chancery, over the past 20 years the bust has undergone recurring maintenance treatments carried out with traditional methods and materials. (Annual and bi-annual maintenance treatments consisted of the removal of the loose superficial deposits by soft bristle brush complemented, when necessary, by rinsing with a 3% solution of the surfactant Tween 20 (IMAR) in deionized water. On two occasions, in 2001 and in 2017, deeper cleaning was carried out by means of cellulose poultice cleaning with a saturated solution of ammonium carbonate, with a dwell time of three to five hours.) In spite of the application of different cleaning procedures, the marble continued to show permanent discoloration, consisting of an unevenly distributed grayish alteration, mainly on the front part of the bust; more concentrated on the cheeks, nose and chin, and less so on the neck, neckline and dress. In 2021 the Embassy’s Cultural Heritage Office sought diagnostic services to perform non-invasive analysis aimed at identifying the nature and cause of the chromatic alteration, and to define possible cleaning methods using sustainable and non-toxic products.

2. Materials and Methods

2.1. Non-Invasive Preliminary Analysis

In order to define the composition of the chromatic alteration, multiple non-destructive analyses were performed on the sculpture. Firstly, the surface of the artwork was examined through multispectral imaging to detect the presence of extraneous materials. UV and IR reflectography was performed with a Madatec[®] multispectral imaging system, comprising: a Samsung NX500 28.2 MP BSI CMOS camera; Hoya Filter UV&IR cut 52; Baader U-Filter 60 nmHBW/320–380 nm; F-PRO MRC Yellow 495; high-pass IR filter 760 and 850 nm cut; and Madatec[®] light sources at 365 nm model CR230B-HP for UV fluorescence, and 440 nm model CR230-440 for VIL and VIVL. With IR source, natural and artificial radiation from the building was exploited. Due to the architectural configuration of the space, it was impossible to completely darken the room during the procedure. This causes the fluorescence color to be altered, preventing a full understanding of the substance’s identity; for this reason, a further multi-analytical approach is necessary.

Secondly, for a better understanding of the superficial color variation on the observed areas, spectro-colorimetric analysis was carried out. The instrument used was a Konica Minolta’s CM-2600d portable spectrophotometer with an 8 mm aperture lens and three Xenon light bulbs. Spectra were collected with a 0.1% standard deviation and the simultaneous acquisition in SCI (specular component included) and SCE (specular component excluded) modes. Spectra were acquired in the visible region (400–700 nm), and the color was defined using the CIE Lab color space coordinates L^* , a^* , b^* .

To define the chemical composition of the alteration, Raman spectroscopy and reflectance spectroscopy (UV-Vis-NIR) were used. Since no organic compounds were revealed during the observations with the imaging system, Raman spectroscopy proves to be a more suitable technique than IR spectroscopy.

A QualitySpec Trek Portable Vis-NIR spectrometer was used to identify possible organic materials present on the surface, using Spectral Range 350 to 2500 nm.

The Raman spectrometer was a QE Pro-Raman from Ocean Insight equipped with a 785 nm laser with a 0 to 400 mW power range, 0 to 4000 cm^{-1} Raman shift and 10 to

14 cm⁻¹ resolution. The spectra were collected using a power of 50 to 150 mW to avoid any laser-caused effects on the surface.

For the identification, Raman spectra were compared with those in the RUFF online database [<https://rruff.info> accessed on 30 March 2022]. The reflectance spectrometer was a Qualityspec[®] Trek with a halogen lightbulb that allows an acquisition range from 350 to 2500 nm (vis-NIR) with a resolution of 3 nm until 700 nm, 9.8 nm from 700 to 1400 nm and di 8.1 nm from 1400 to 2500 nm. Collected spectra were interpreted using the USGS (United States Geological Survey) online database (<https://crystal.usgs.gov/speclab/QueryAll07a.php> accessed on 30 March 2022). Figure 1 shows the measure points for the aforementioned techniques.

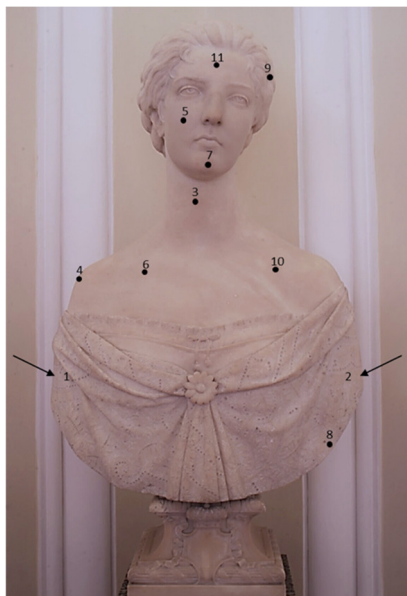


Figure 1. Measure points map. The arrows indicate the points on the back of the statue (points 1 and 2).

The synthesis of diagnostic iter and the areas where the spectra were collected are reported in Table 1.

Table 1. Measure points summary, corresponding statue areas and analytical techniques used.

N.	Statue Areas	Analytical Techniques		
		Colorimeter	Raman Spectroscopy	Reflectance Spectroscopy
1	Back left	X	X	X
2	Back right	X	X	X
3	Neck	X		X
4	Left shoulder	X		X
5	Left cheek	X	X	X
6	Left chest	X		X
7	Chin	X	X	X
8	Dress	X	X	X
9	Hair		X	
10	Right chest			X
11	Forehead			X

2.2. Cleaning Tests

The tested cleaning systems are reported in Table 2.

Table 2. Tested cleaning systems.

ID	Product	Manufacturer
1	Polar Varnish Rescue GEL	YOCOCU APS
2	Alkoxyde based surfactant	Sigma Aldritch
3	GLDA (5% in H ₂ O <i>w/v</i>)	Nouryon
4	Disodium EDTA (5% in H ₂ O <i>w/v</i>)	Sigma Aldritch
5	Politect base [®]	Politect
6	Deionized water as reference	-

One area, treated with deionized water only, was used as a reference. Specifically, Polar Varnish Rescue is a new green low-toxic mixture of solvents developed by YOCOCU APS; the second product used is an alkoxyde-based surfactant; disodium EDTA is a chelating agent, specifically a disodium salt of ethylenediaminetetraacetic acid; GLDA is a chelating agent based on L-glutamic acid [30]; and Politect[®] Base is a formulation based on polyvinyl alcohol, plasticizers, rheology modifiers and additives in aqueous solution. The latter is a gel that can be removed in a single solution by peeling once the film is formed, without requiring further cleaning to remove residues. The effectiveness of the treatments was evaluated by a Dinolite[®] AM411-FVW, 1,3 Mpx (1280 × 1024), 10–70× and 200× magnification, UV + white led light source USB digital microscope and DinoCapture 2.0 software to observe the surface color and morphology before and after the treatment. Criteria for the evaluation of the best system are the following:

- Ability to effectively remove the particulate matter that has penetrated the porosity;
- Toxicological and chemical-physical properties in compliance with the principles of green chemistry;
- Selectivity towards the material to be removed to preserve the surface of the artwork;
- Ability to achieve maximum removal of the particulate matter by operating in the least invasive way possible;
- Easy application and ability to control the cleaning method.

Application Method

According to Macchia et al. [30], 25 mL of Polar Varnish Rescue was gelled using 5% (*w/v*) Klucel G and then applied on the base of the bust by interposing a sheet of Japanese paper to avoid gel residues on stone surface. In order to obtain comparable results, 25 mL of deionized water, alkoxyde surfactant, EDTA and GLDA were supported in 5 g of cellulose pulp. Disodium EDTA can be used at a concentration between 2% to 15%, but a lower concentration must be considered when working with limestone as this chemical compound can chelate calcium ions. For this reason, a 5% disodium EDTA solution in water was applied [31,32]. GLDA was prepared as in Macchia et al. [33] at 5% concentration, and brought to pH 9 with acetic acid. Deionized water and alkoxyde surfactant were directly suspended in cellulose pulp. All treatments were applied on the statue base interposing a sheet of Japanese paper and covered by a polyethylene layer. All tests were removed according to the slowest action time (EDTA) [34], after 1 h and 10 min.

For the Politect[®] Base gel, manufacturer application instructions were followed. The product was directly applied on the base of the bust. After 30 min, a second thicker layer was applied on the first one. After 24 h, the film was peeled off from the surface. After the cleaning tests, all the treated areas were further cleaned with deionized water, and then with dry cotton swabs, to remove the product residues. The different products were applied in delimited areas at the base of the bust (Figures 2 and 3).



Figure 2. Cleaning areas selection and delimitation.



Figure 3. Product application on the base as described in Table 3.

Table 3. CIELab coordinates on the measuring points and color simulation (c.s.) in the Hex color system.

Point	1	2	3	4	5	6	7	8
Description	Left back	Right back	Neck	Left shoulder	Left cheek	Left chest	Chin	Dress
C.S.	#C1C0BE	#BDBCB9	#A39F97	#A09A8E	#A29D95	#A6A298	#A19C92	#837D74
L*	77.84	76.3	65.81	63.83	65.11	66.6	64.68	52.83
a*	−0.05	−0.03	0.33	1.07	0.71	0.23	0.6	0.75
b*	1.38	1.63	4.77	6.88	4.85	5.72	6.06	5.85

3. Results

3.1. Non-Invasive Preliminary Analysis

Calcite mineral only fluoresces in certain conditions, and in the case of marble does not fluoresce at all. Due to the architectural setting of the staircase (the windows being located high up and out of reach), it was impossible to obtain a completely dark room during the UV light measures. Still, the imaging technique allowed to obtain information on the surface status. Under UV light, some fluorescent areas were revealed:

- Areas with a blue induced fluorescence could be related to superficial structural variations from calcium carbonate polymorphs. As Toffolo et al. showed in their work [35], calcium carbonate polymorphs like aragonite and pyrogenic calcite in fact have a visible fluorescence in the blue region (Figure 4a,b). Also, by varying light angles, the analysis showed different fluorescence colors, thus revealing the inorganic nature of the substance;
- A blue induced fluorescence located on the back and front of the sculpture reveals dripping residues of an unidentified product (Figure 4c,d);
- A yellowish induced fluorescence around the base corner may be related to an organic adhesive used in previous reintegration work (Figure 4e).



Figure 4. Details of visible induced fluorescence areas under UV light. (a) Head: Hair and eye. UV fluorescence of calcite polymorphs; (b) Head: face area. UV fluorescence of calcite polymorphs; (c) Body: drippings. UV fluorescence; (d) Back: drippings. UV fluorescence; (e) Base: adhesive UV fluorescence.

Fluorescence was also detected in differently colored areas of the statue, which are unrelated to the examined dark areas.

With IR reflectography, images with a stronger contrast between darker and lighter areas were obtained. This allowed the clear definition of the areas affected by the darkening, meaning the composite has a strong response to IR radiation (Figure 5c).

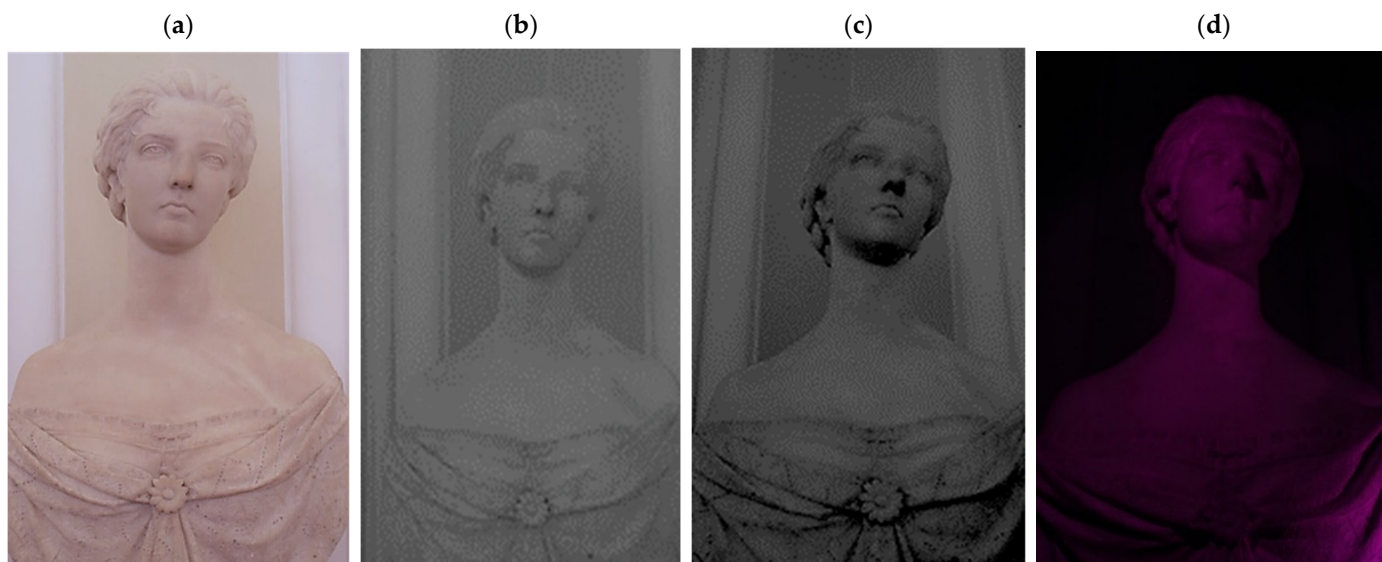


Figure 5. IR and UV reflectography acquisitions compared to the picture under visible light. (a) Visible light; (b) IR reflectography (750 nm); (c) IR reflectography (850 nm); (d) UV reflectography.

Colorimetric measurements were acquired in points 1 to 8. As points 1 and 2 were significantly lighter than other areas, it is possible to assume that these are probably the closest to the original stone color, considering the other areas studied; for this reason, they were chosen as a color reference for the specific material. Table 3 shows the measurements acquired with the instrument. The relatively consistent decrease in the L^* value in point 8 is noticeable in comparison with the reference points, while a less conspicuous variation involves the other points. Lower values of L^* denote a darkening of the surface color. Further, the variation of b^* and a^* coordinates towards higher values means the color is shifting towards yellower tones. The difference can be immediately observed thanks to the color simulation (shown in Table 3) associated with the respective hexadecimal color code, a 6-digit unique code where each pair of symbols represents the color values for red, green and blue.

Previous results are also confirmed by the spectra in Figure 6, where a decrease in reflectance of around 20–26% for points 3 to 7 and around 35% for point 8 can be observed, highlighting the presence of darker areas.

The Raman spectroscopy data acquired in points 1, 2, 5, 7, 8 and 9, along with all spectra, can be found in Appendix A. The identification was made possible by matching the spectra collected with those in the RUFF database (<https://ruff.info> accessed on 30 March 2022). All spectra are typical of calcium carbonate (RUFF R040070), the main component of marble (Table 4). Calcium carbonate typically exhibits a strong band at 1086 cm^{-1} , which is assigned to the C–O symmetric stretch vibration, and a weak band at 712 cm^{-1} , assigned to a plane-bending vibration of CaCO_3 [36,37]. No fluorescence was observed, and no other minerals and compounds were detected. Given the absence of other crystal phases, it can be deduced that a pure (or almost pure) white marble was used for the artwork. This can also be deduced from microscopic observation of the surface with Dinolite[®]. The stone shows a granoblastic saccaroid structure with a very fine grain (<1 mm) typical of marble [38] (Figure 7).

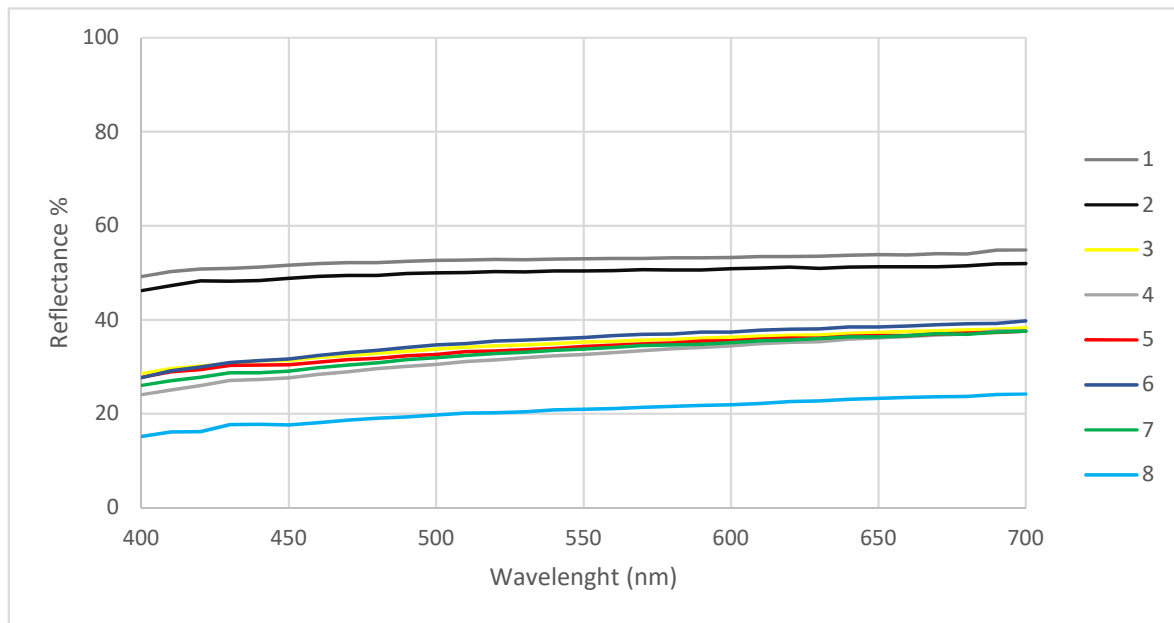


Figure 6. Reflectance spectra in the visible range collected in the different areas of the statue.

Table 4. Most important Raman bands of the collected spectra, identified compound, and reference spectra and bands (RUFF).

Statue Areas	Sample Bands (cm ⁻¹)
Left back	280; 711; 1085
Right back	282; 710; 1085
Left cheek	281; 712; 1085
Chin	282; 713; 1085
Dress	281; 712; 1085
Hair	281; 712; 1085

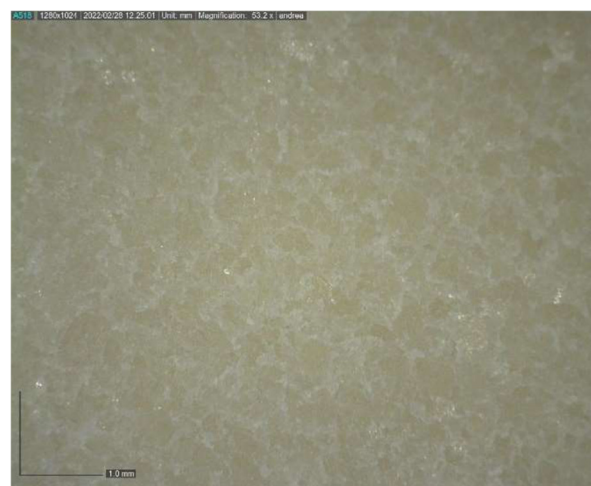


Figure 7. Image at 53.2× magnification of the surface.

Reflectance spectroscopy spectra confirm the results obtained by Raman spectroscopy as well. The acquisition was carried out on points 1 to 8, 11 and 12, and spectra are available in Appendix B. All spectra match with those of calcium carbonate (USGS Calcite WS272) (<https://crystal.usgs.gov/speclab/QueryAll07a.php> accessed on 30 March 2022), and no other

compounds were identified. Reflectance IR spectra of calcium carbonate have characteristic bands at around 1435 cm^{-1} due to the asymmetric stretching of CO_3 groups, a 1875 cm^{-1} band attributable to the combination modes of symmetric stretching and deformation of CO_3 groups, and a band at around 2400 cm^{-1} due to symmetric and asymmetric deformation of CO_3 groups, while the other signals are overtone bands (Table 5) [39].

Table 5. Most important Reflectance spectroscopy bands of the collected spectra, identified compound, and reference spectra and bands (USGS).

Statue Areas	Sample Bands (nm)
Left back	1449; 1565; 1650; 1757; 1875; 1994; 2153; 2337; 2402
Right back	1453; 1565; 1650; 1755; 1875; 1994; 2157; 2337; 2400
neck	1475; 1567; 1650; 1757; 1875; 1996; 2157; 2335; 2400
Left shoulder	1459; 1565; 1648; 1757; 1875; 1994; 2155; 2337; 2400
Left cheek	1457; 1565; 1648; 1757; 1875; 1994; 2155; 2337; 2402
Left chest	1461; 1565; 1648; 1757; 1875; 1996; 2155; 2337; 2398
Chin	1465; 1567; 1650; 1757; 1875; 1996; 2155; 2337; 2400
Dress	1455; 1565; 1650; 1757; 1875; 1996; 2157; 2339; 2396
Right chest	1451; 1567; 1656; 1757; 1875; 1948; 1994; 2157; 2339; 2402
Forehead	1449; 1567; 1654; 1759; 1875; 1994; 2157; 2337; 2404

3.2. Cleaning Tests

The use of DinoLite[®] (Table 6) and macroscopic observation (Figure 8) made it possible to define which product best meets the requirements expected from the cleaning system. Based on the criteria used for solvent selection, GLDA and Politect[®] Base showed the best results. Using only the peeling effect, Politect[®] Base showed a good ability to remove most of the particulate matter on the surface and inside the porosity of the marble. The GLDA was just as effective. It allowed to obtain a uniform appearance of the surface, removing the gray stains that covered it. The Polar Varnish Rescue GEL, the alkoxyolate-based surfactant and the deionized water did not show the same effectiveness, while the disodium EDTA proved to be more aggressive than the GLDA, giving rather non-homogeneous results.

Table 6. Dinolite[®] images of the areas before and after treatment.

	Before Cleaning	After Cleaning
1-Polar Varnish Rescue GEL		

Table 6. Cont.

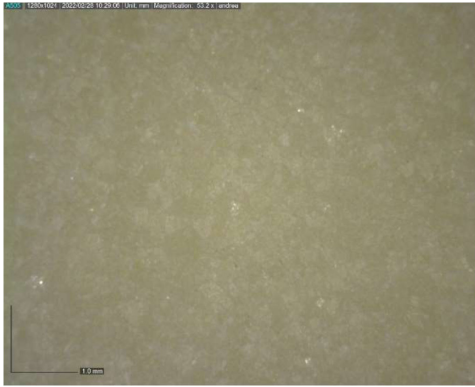
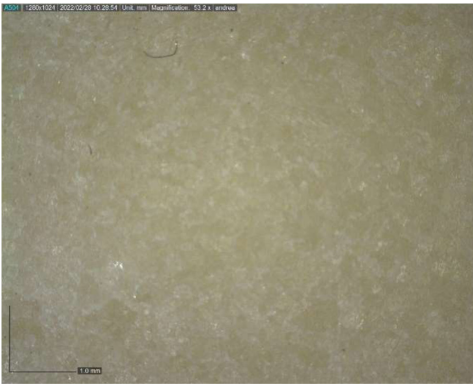
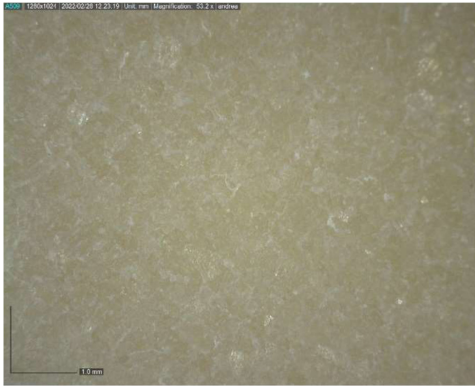


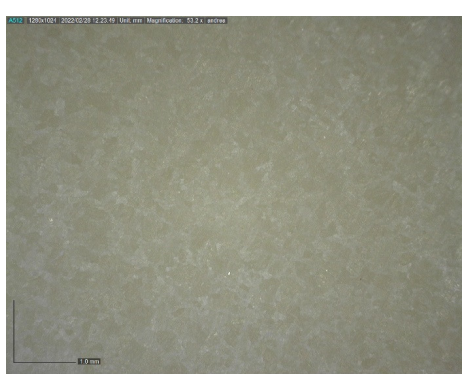
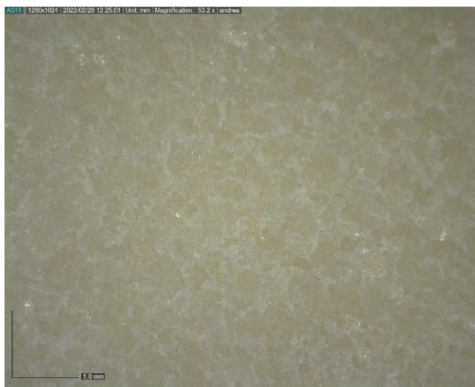

	Before Cleaning	After Cleaning
2-Alkoxyated-based surfactant		
3-GLDA		
4-EDTA		
5-Politect base		



Figure 8. Photographs of the surfaces after treatment.

The comparison between the images acquired using DinoLite[®] before and after the cleaning tests confirm that GLDA and Politect[®] Base show the greatest cleaning power (Table 6). All the images collected show that the original morphology of the marble surface has been preserved.

The obtained results were also measured by spectrorimetry (Table 7). Measurements before and after cleaning were acquired in five different points per area, averaged and compared. The analysis confirmed what had already been seen, with DinoLite[®]: Politect[®] Base demonstrating the best action, followed by GLDA and then EDTA, all with higher L* values than references. This corresponds to lighter and whiter color tones. On the contrary, areas cleaned with Polar Varnish Rescue and the alkoxykated surfactant showed poor results as L* values are close to reference and b* values are even higher, meaning a yellower color.

Table 7. Colorimetric measurements after cleaning tests. All measures are averaged. SDL* = 2; SDA*, SDb* = 0.5.

	Polar Varnish Rescue		Alkoxyated-Based Surfactant		GLDA		EDTA		Politect [®] Base	
	Before	After	Before	After	Before	After	Before	After	Before	After
L*	78.89	79.21	77.20	77.45	78.53	83.88	76.33	78.44	77.10	84.1
a*	1.04	1.11	1.15	1.07	1.02	−0.04	1.11	−0.07	1.02	0.83
b*	2.90	2.61	2.60	2.71	2.40	0.81	2.44	3.63	2.63	1.63

4. Discussion

A completely non-invasive analytical approach was used in order to discover the nature of gray discoloration on the marble bust representing Queen Margherita di Savoia at the U.S. Embassy in Rome, for cleaning purposes. At first, multispectral imaging was performed to verify the presence of organic superficial residues. The technique showed interesting aspects about the structural composition of the marble by revealing a regional UV fluorescence caused by the presence of calcium carbonate polymorphs like aragonite or pyrogenic calcite [35]. The technique identified also identified traces of drippings of an extraneous material on the back of the sculpture, which cannot be identified without further analysis, and a visible reintegration highlighted by the yellowish fluorescence of an adhesive of organic nature. Under IR light (850 nm), darkening of the discoloration becomes noticeably visible under the chin and dress folds. This means that the compound is reactive under IR radiation. Color measurement of the surface revealed an objective darkening and yellowing of the marble at different grades based on the area investigated. An important difference in color can be observed between the front and the back of the statue, with darker

tones on the front. It is also noticeable that the darkening is located in creases and sloping surfaces like the nose, neck, chin, and particularly in the dress folds. Raman and reflectance spectroscopy data both gave information about the stone material composed of calcium carbonate. No other mineral phases were detected by Raman and reflectance spectroscopies, nor by microscopical observation. Further, extraneous materials (patinas, waxes, protection materials, etc.) [12] and evidence of weathering (gypsum, calcium oxalates) [40] were not observed. Other analysis like XRD could clarify the exact mineral composition on the stone, and further investigation with a FTIR analysis could better detect the presence of extraneous material, but this was not taken into consideration as it would require sampling. Considering all of the information acquired, it is possible to hypothesize that the darkening of the stone is caused by a dust and particulate matter deposition inside the creases and sloping surfaces that penetrated the marble porosity, since environmental depositions are usually composed of carbonaceous particles reactive to IR radiation. This can be explained by the location, the palace grand staircase, which connects indoor and outdoor spaces, is subject to high volumes of –traffic and is frequented daily by numerous persons. The entrance door, which is original and made of a tall wooden frame with glass panes, does not perfectly seal the entryway. For these reasons, a considerable amount of particulate matter is transported inside the room and moved by upward and downward currents. The reason for which the bust is unevenly stained might be partly due to its surface morphology, and partly because of the different levels of porosity of the marble, possibly depending on its varying conservation condition. A similar case was that of the Taj Mahal dome, frequently subject to discoloration. A study was carried out on the air quality of the Agra region finding that the main cause of the marble darkening was due to depositions of light absorbing particles from aerosols like dust and black and organic carbon [5,6]. To validate this hypothesis, further studies on the patina composition are needed, such as elemental analysis (to check if key chemical elements are present), non-destructive analysis (such as a portable XRF); or, if there is the opportunity to take samples, a SEM-EDS analysis could be performed to study the morphology of the deposition, as well as to double-check for the presence of calcium oxalates (frequently responsible for marble discoloration) [40,41], gypsum (related to the weathering of limestone and responsible, together with air pollution, for black crust formation) [1–4] and biological patinas [11–13].

Five products were selected for the cleaning tests based on their toxicological and sustainable properties according to green chemistry principles [42]. In terms of cleaning efficiency and sustainability, Politect[®] Base was evaluated as the best product. Since Politect[®] is a water-based and solvent-free product, the cleaning action is due to its peeling effect, and its high selectivity for the materials to be removed is based on its chemical inertness towards marble. Good results were also obtained by the chelating agent GLDA, also a green product, and equally respectful of the surface since it can dissolve calcium carbonate only at high temperatures [43–45].

On the contrary, EDTA, also a chelating agent, proved to be too aggressive and altered the surface morphology. EDTA was in fact already cited as a dissolving agent for calcite since it affects the crystalline lattice removing calcium cation [46]. Moreover, EDTA is a persistent compound in soil and water, harmful if inhaled and noxious for internal organs, which is why it does not comply with green chemistry principles [47,48]. Solvents (Polar Varnish Rescue and water) and surfactants (alkoxylated) could not remove the discoloration. The most probable reasons are that the polarity of these products does not match that of the material to be removed, or that their action is limited to the surface and could not penetrate the marble porosities.

5. Conclusions

The analysis described in this paper allowed to detect and objectively measure color differences of various artwork areas. Spectrocolorimetry data highlight conspicuous color differences between visibly lighter and darker areas, with a reflectance decreasing, in some cases, above 30%. Raman and reflectance spectroscopies were used to characterize the stone

material that is composed of calcium carbonate. Multispectral imaging information instead revealed superficial compounds in the form of isolated drippings, revealing the presence of a product from a previous restoration and structural inhomogeneity of the marble due to the presence of calcium carbonate polymorphs (aragonite and/or pyrogenic calcite). Also, IR reactive depositions were detected mainly in the creases of the relief. Since this analysis did not reveal any traces of marble weathering and compositional differences of the surface able to justify marble discoloration, it is assumed that consistent deposition of dust and particulate matter penetrating marble porosity is responsible for the surface darkening, although further studies on the composition of the deposits should be carried out.

The cleaning tests performed on the bust of Queen Margherita allowed to identify the best solution for the removal of the particulate matter on the surface and inside the porosity of the marble. In terms of effectiveness and preservation of the original material, the best results were obtained with GLDA, a chelating agent, and Politect[®] Base, a gel based on polyvinyl alcohol. The Politect[®] Base was used as is. It owes its cleaning action to the peeling effect during removal. Given its poor interaction with the original material, it is considered a suitable product to be used for the cleaning of the entire artwork. Instead, the GLDA is recommended in areas where the Politect[®] Base is not sufficiently effective or the peeling effect is not recommended, such as the area corresponding to the lace decoration.

Author Contributions: Conceptualization, A.M. and V.B.; methodology, A.M. and V.B.; investigation, A.M., L.R., I.A.C., H.A. and C.B.; data curation, A.M.; writing—original draft preparation, E.C. and C.B.; writing—review and editing, V.B.; visualization, A.M., E.C., L.R., I.A.C., H.A., C.B. and V.B.; supervision, A.M.; All authors have read and agreed to the published version of the manuscript.

Funding: This research was funded by the U.S. Department of State-Bureau of Overseas Buildings Operations/OPS/Office of Cultural Heritage.

Institutional Review Board Statement: Not applicable.

Informed Consent Statement: Not applicable.

Data Availability Statement: The data presented in this study are available in Appendices A and B.

Conflicts of Interest: The authors declare no conflict of interest.

Appendix A

Raman spectroscopy of measure points.

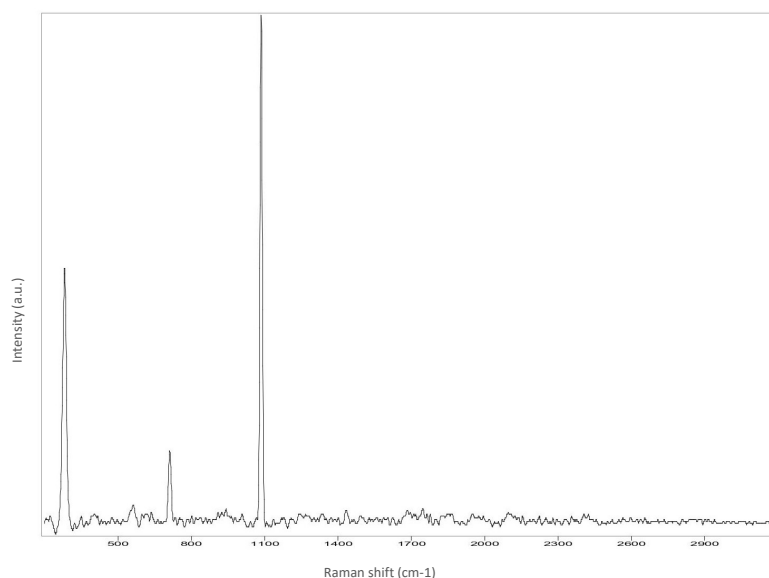


Figure A1. Back-left.

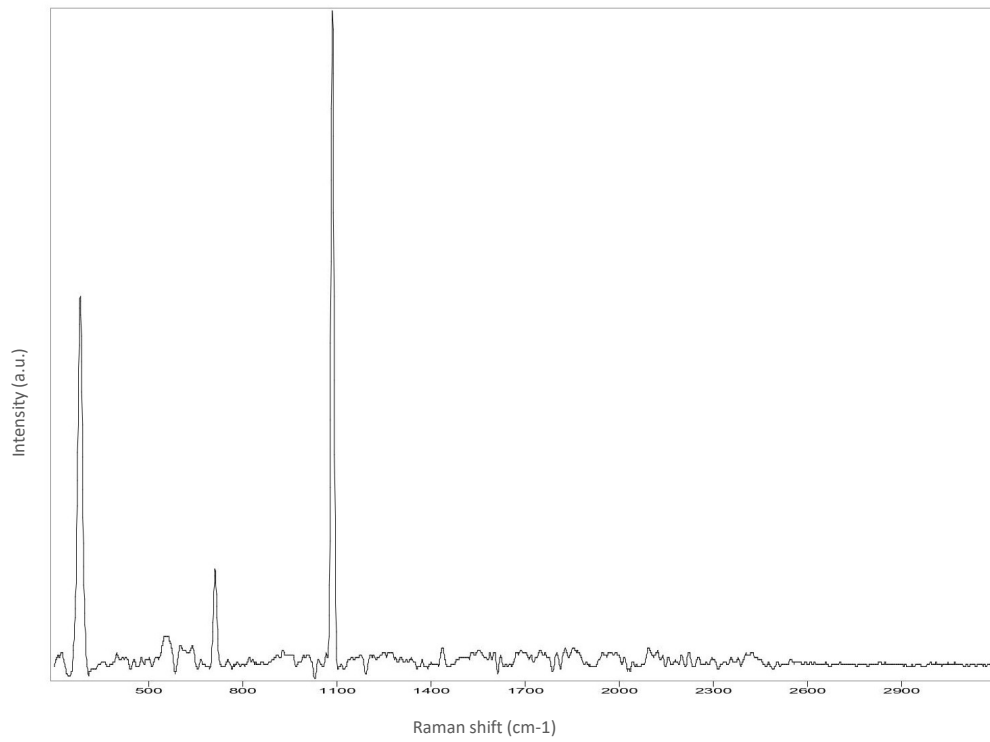


Figure A2. Back-right.

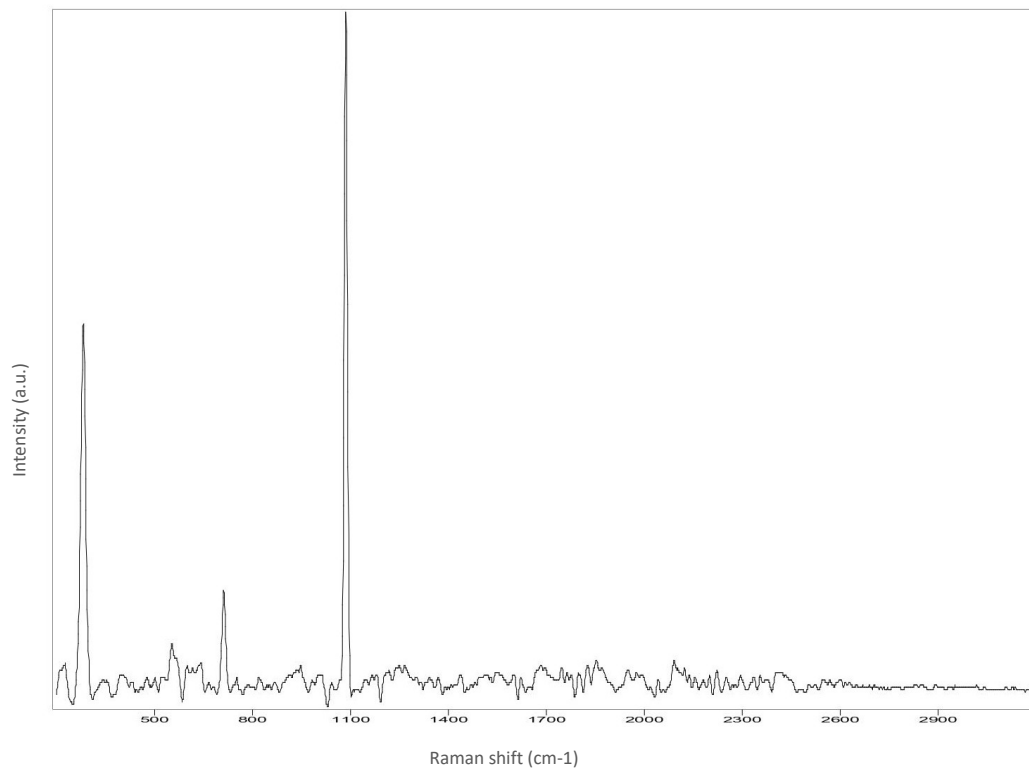


Figure A3. Left cheek.

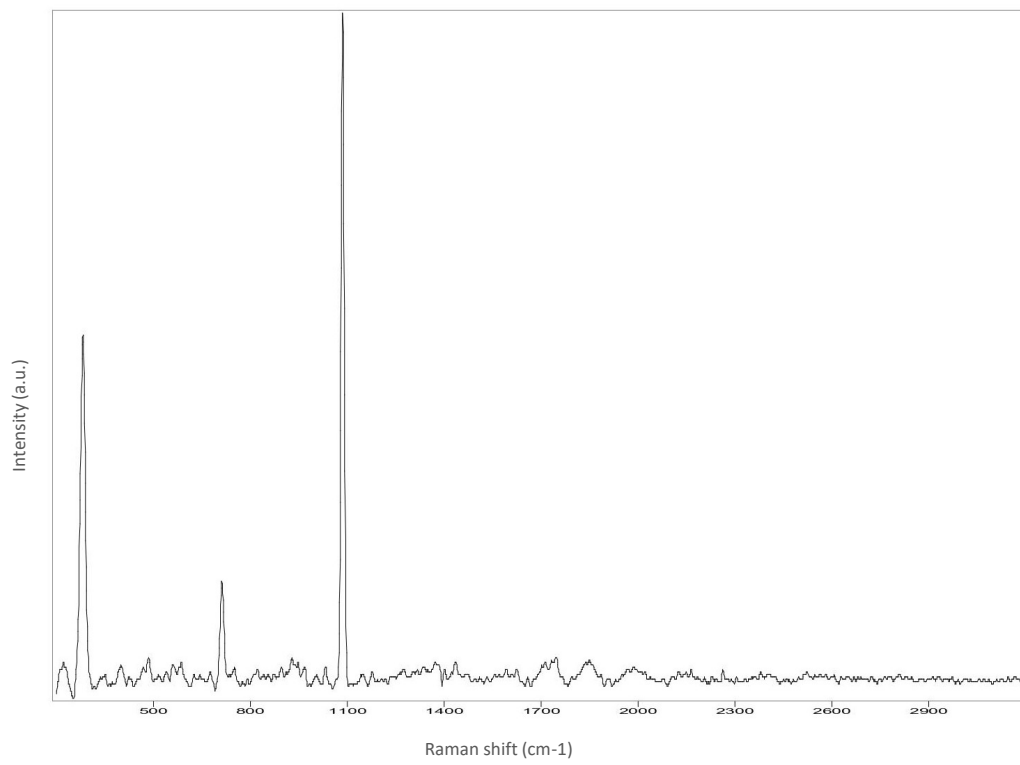


Figure A4. Chin.

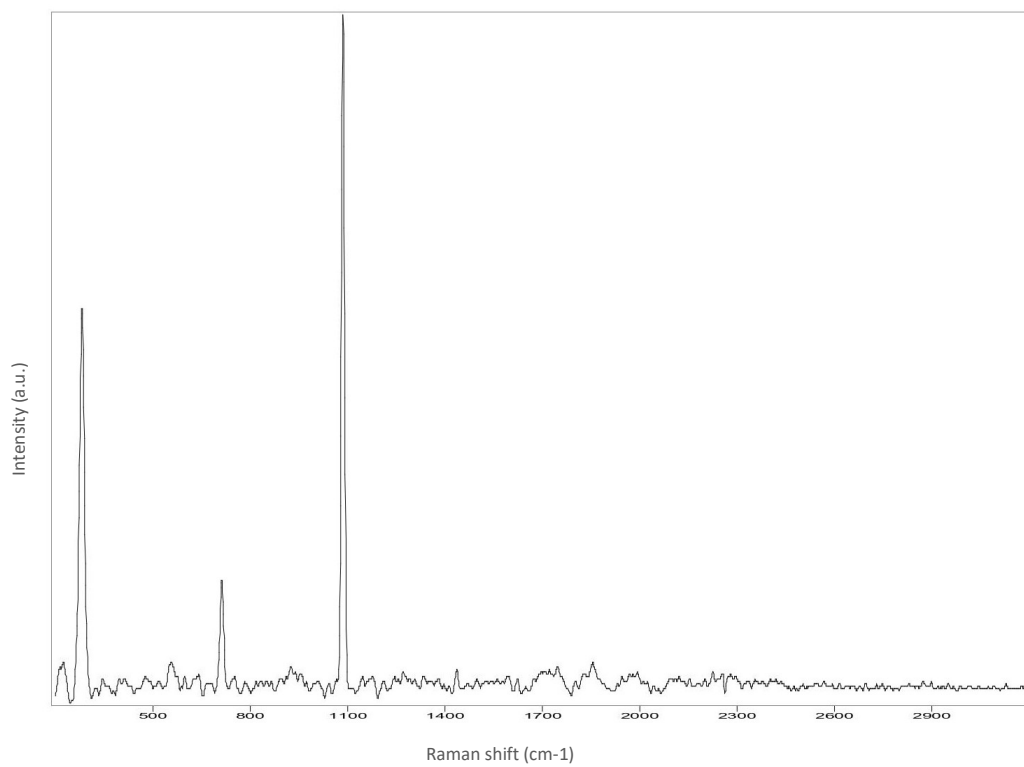


Figure A5. Dress.

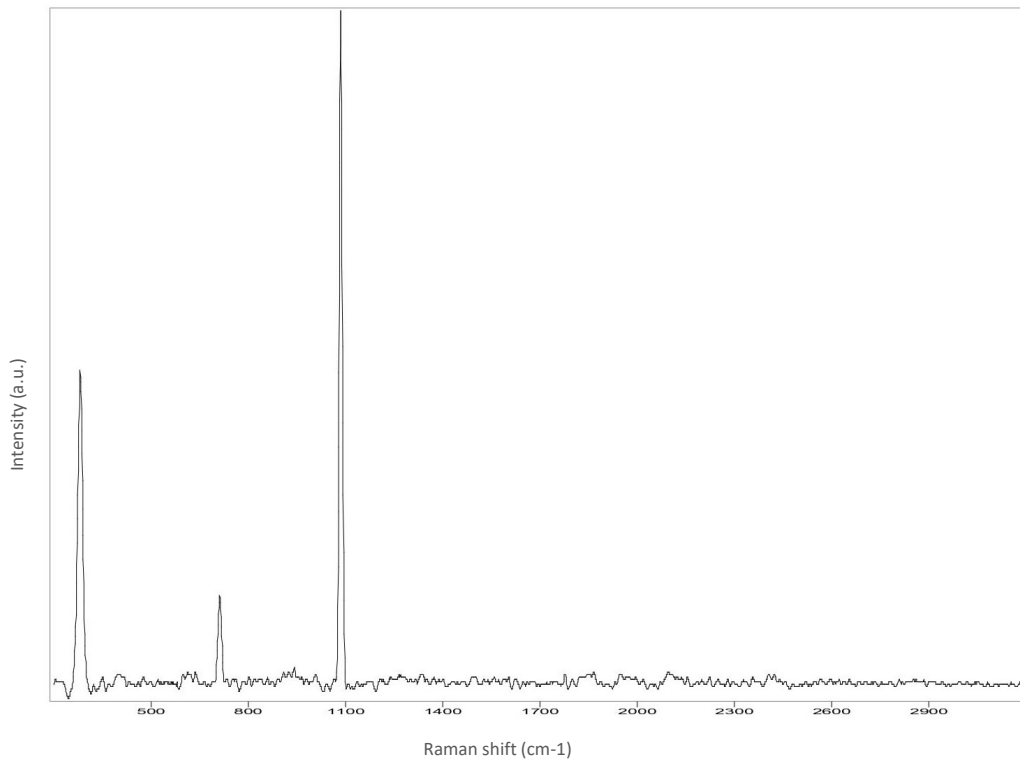


Figure A6. Hair.

Appendix B

UV-vis-NIR Reflectance spectroscopy of measure points.

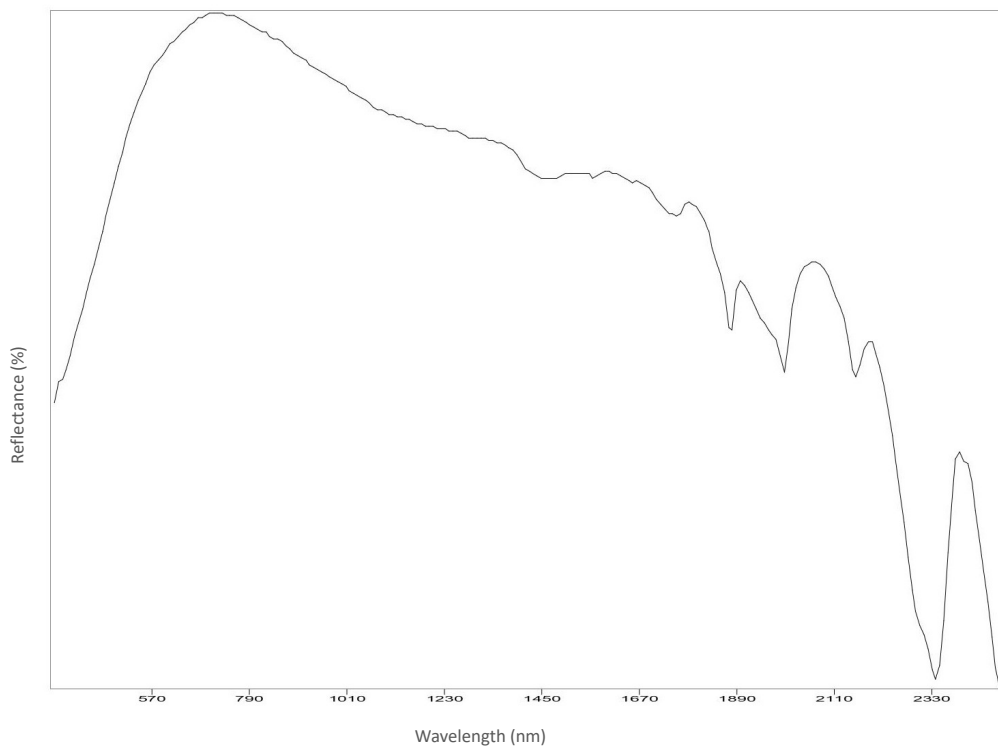


Figure A7. Back-left.

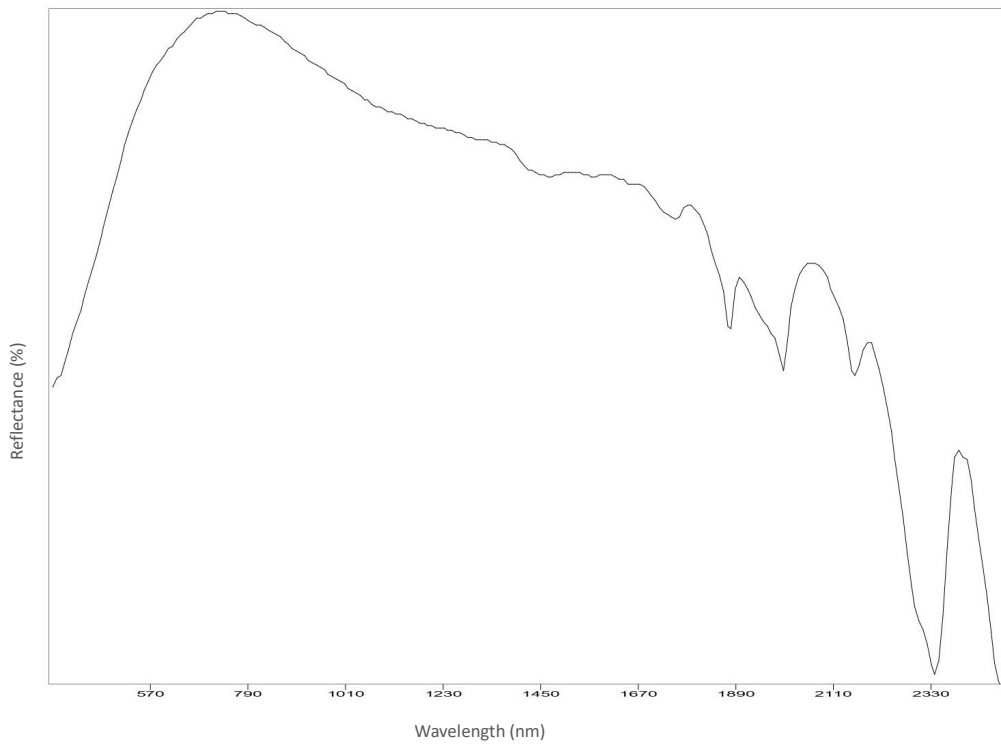


Figure A8. Back-right.

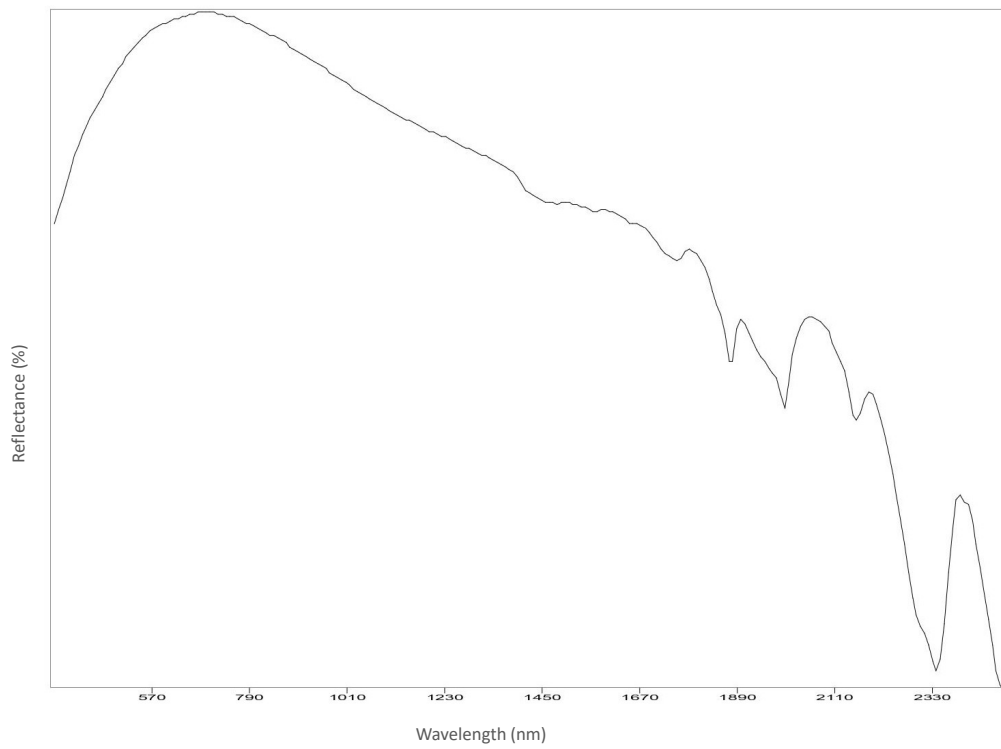


Figure A9. Neck.

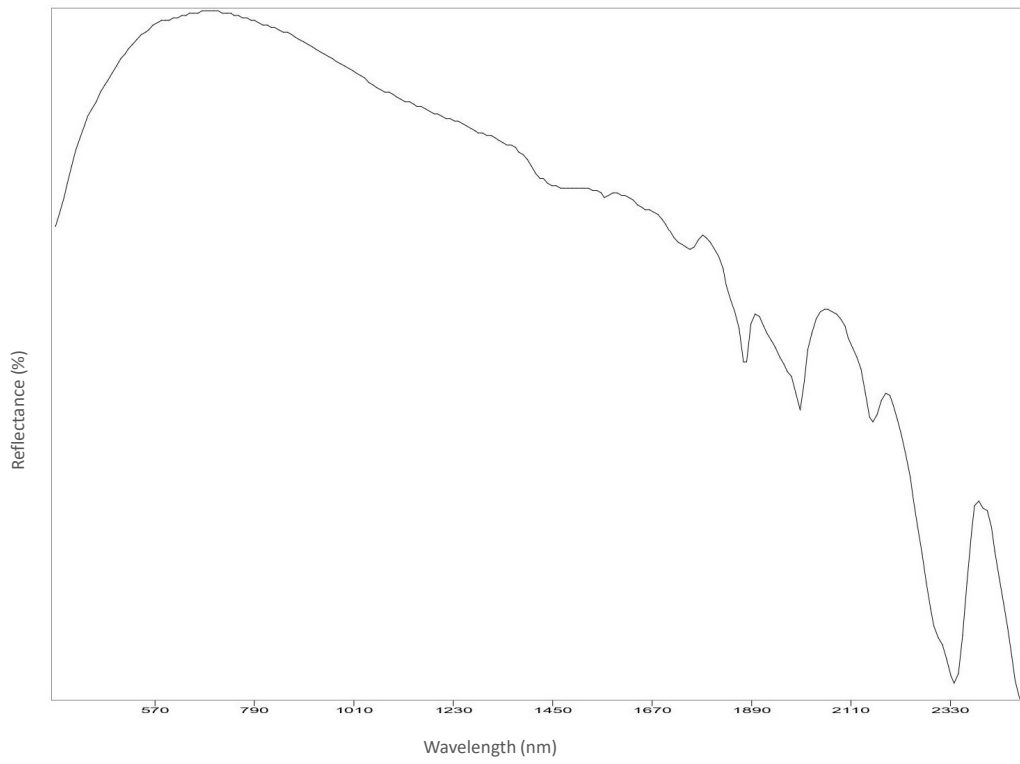


Figure A10. Left shoulder.

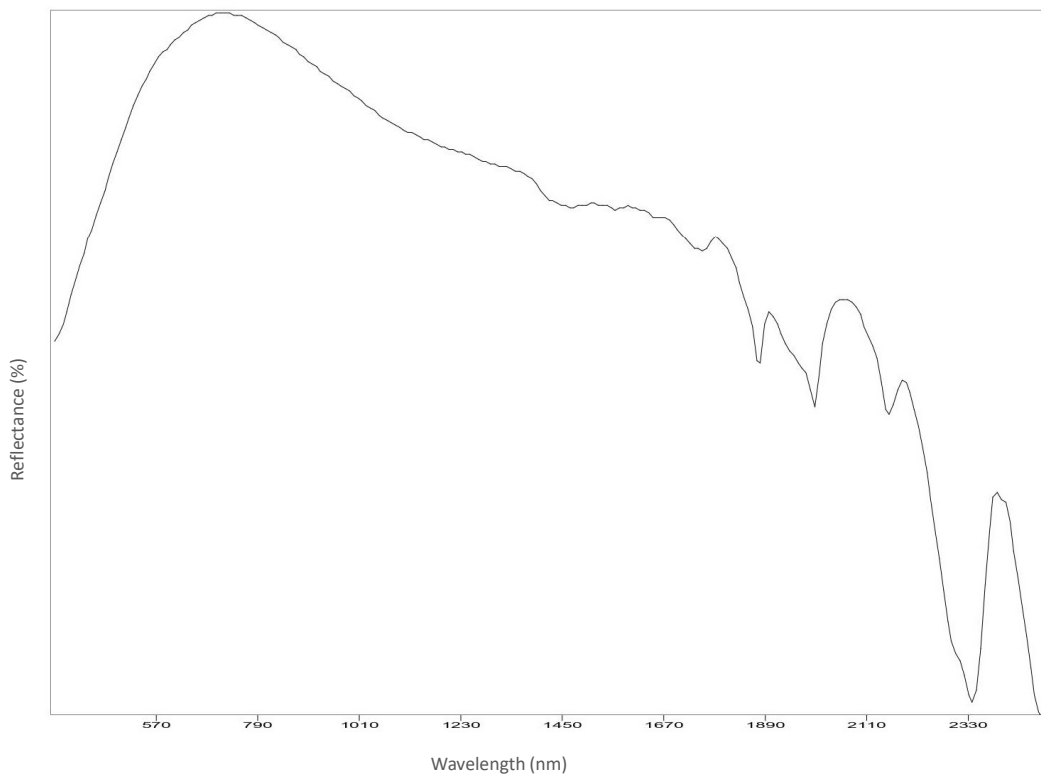


Figure A11. Left cheek.

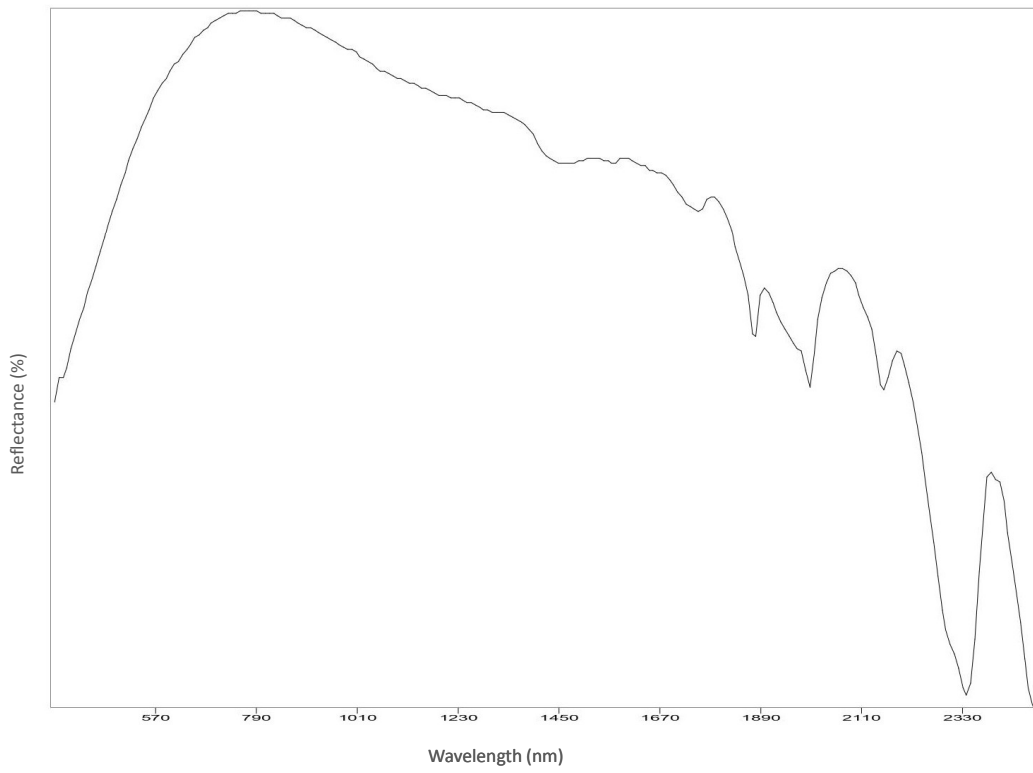


Figure A12. Left chest.

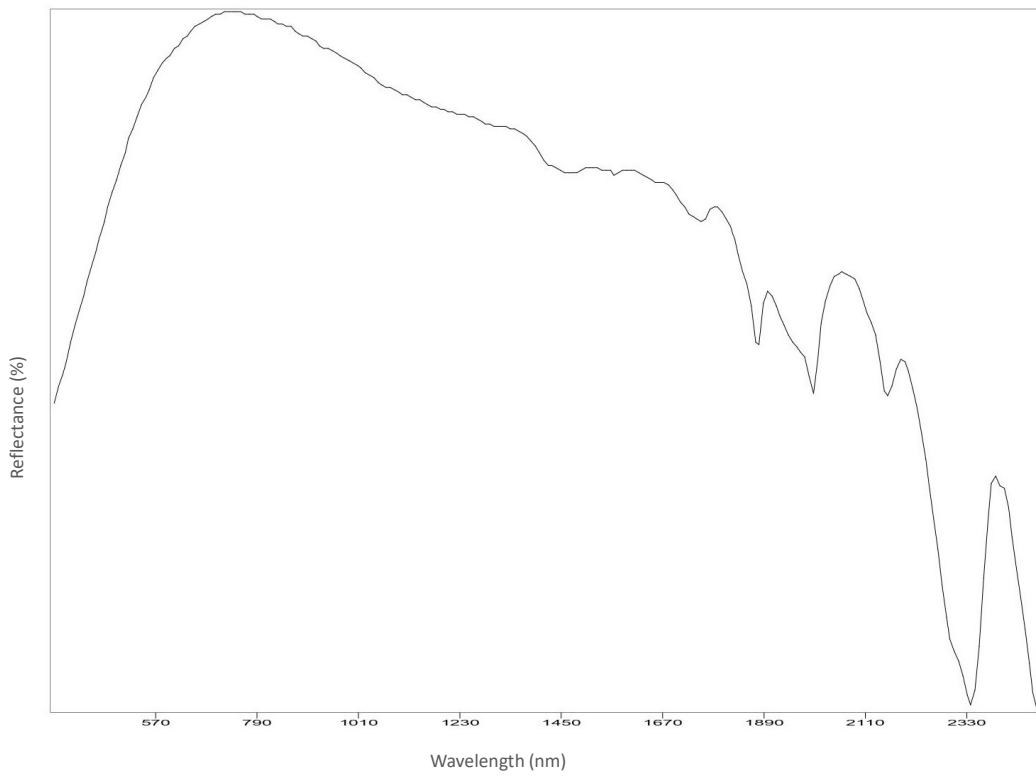


Figure A13. Chin.

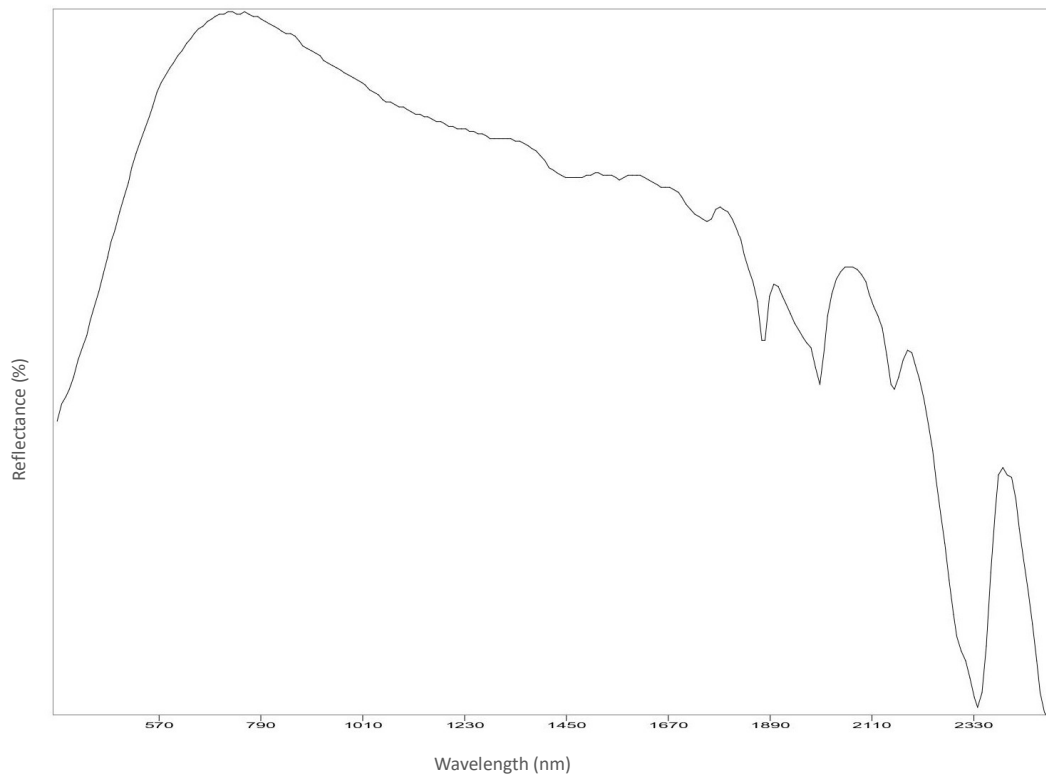


Figure A14. Dress.

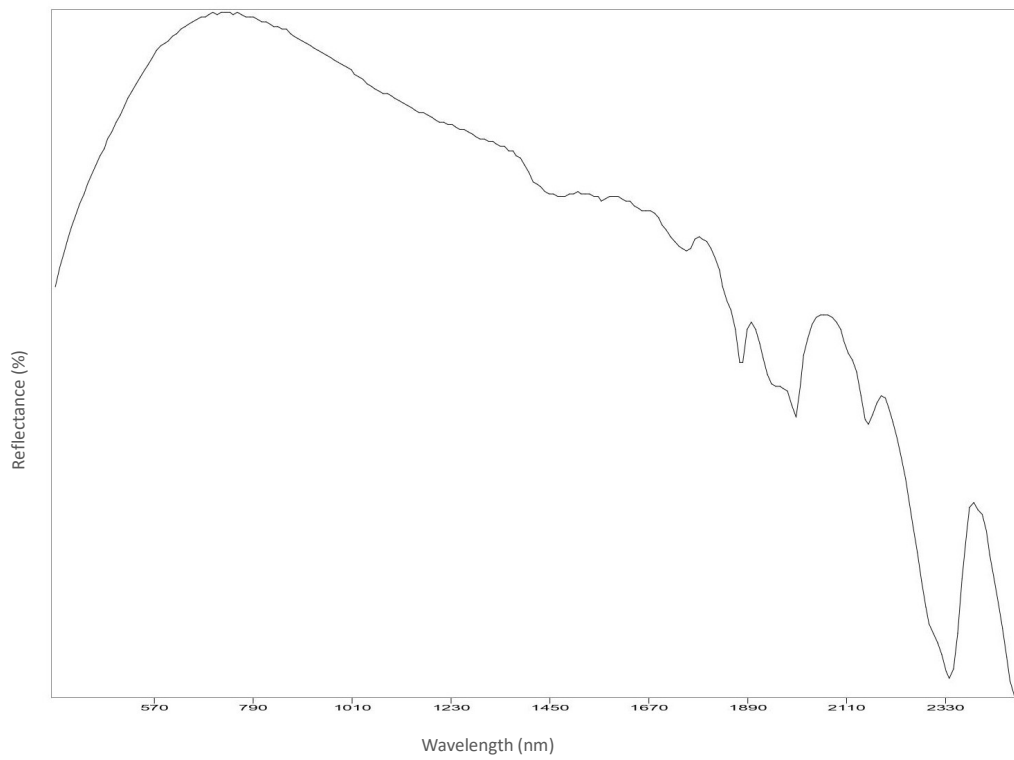


Figure A15. Right chest.

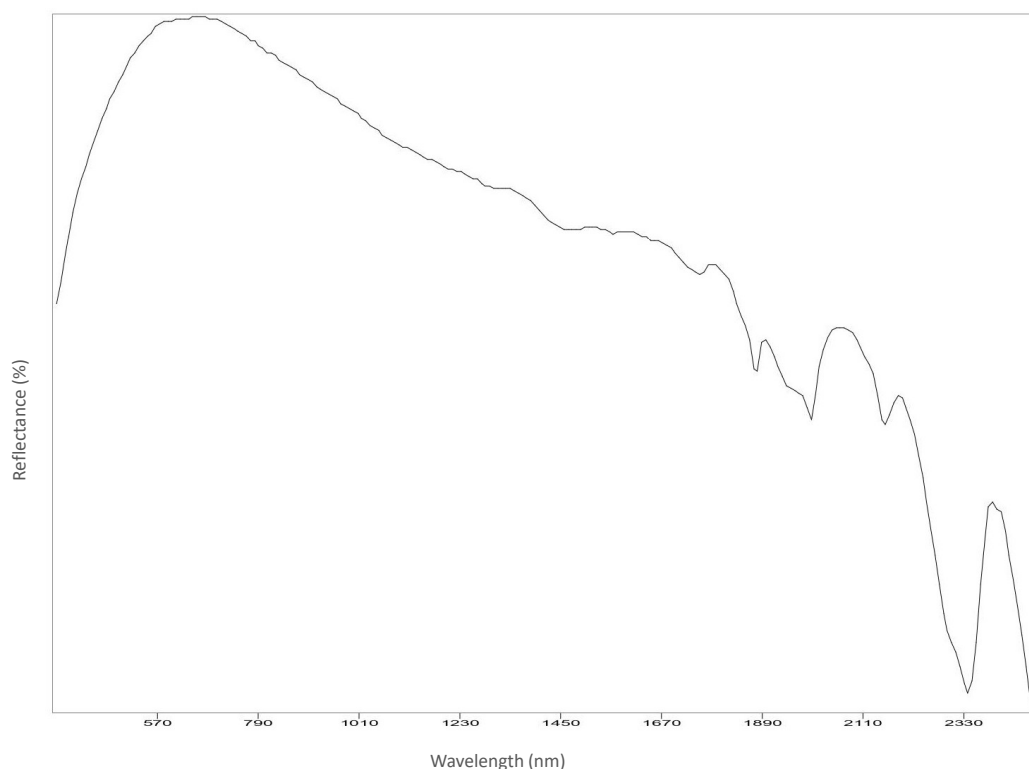


Figure A16. Forehead.

References

1. Maravelaki-Kalaitzaki, P. Black crusts and patinas on Pentelic marble from the Parthenon and Erechtheum (Acropolis, Athens): Characterization and origin. *Anal. Chim. Acta* **2005**, *532*, 187–198. [[CrossRef](#)]
2. Bugini, R.; Tabasso, M.L.; Realini, M. Rate of formation of black crusts on marble. A case study. *J. Cult. Herit.* **2000**, *1*, 111–116. [[CrossRef](#)]
3. Comite, V.; Pozo-Antonio, J.S.; Cardell, C.; Randazzo, L.; La Russa, M.F.; Fermo, P. A multi-analytical approach for the characterization of black crusts on the facade of an historical cathedral. *Microchem. J.* **2020**, *158*, 105121. [[CrossRef](#)]
4. Mitsos, D.; Kantarelou, V.; Palamara, E.; Karydas, A.G.; Zacharias, N.; Gerasopoulos, E. Characterization of black crust on archaeological marble from the Library of Hadrian in Athens and inferences about contributing pollution sources. *J. Cult. Herit.* **2022**, *53*, 236–243. [[CrossRef](#)]
5. Bergin, M.H.; Tripathi, S.N.; Jai Devi, J.; Gupta, T.; McKenzie, M.; Rana, K.S.; Shafer, M.M.; Villalobos, A.M.; Schauer, J.J. The discoloration of the Taj Mahal due to particulate carbon and dust deposition. *Environ. Sci. Technol.* **2015**, *49*, 808–812. [[CrossRef](#)]
6. Arola, A.; Schuster, G.; Myhre, G.; Kazadzis, S.; Dey, S.; Tripathi, S.N. Inferring absorbing organic carbon content from AERONET data. *Atmos. Chem. Phys.* **2011**, *11*, 215–225. [[CrossRef](#)]
7. Funke, A.; Poole, L.; Church, J.; Striegel, M.; Singer, M. The use of medical chelating agents for the removal of iron stains from marble. *Objects Specialty Group Postprints* **2017**, *24*, 235–249.
8. Kamally, H.A. Orange, Yellow, Brownish Stains and Alteration on White Marble at El Montazah in Alexandria, Egypt. *Int. J. Archit. Herit.* **2021**, *15*, 1942–1958. [[CrossRef](#)]
9. Sansonetti, A.; Bertasa, M.; Corti, C.; Rampazzi, L.; Monticelli, D.; Scalarone, D.; Sassella, A.; Canevali, C. Optimization of Copper Stain Removal from Marble through the Formation of Cu (II) Complexes in Agar Gels. *Gels* **2021**, *7*, 111. [[CrossRef](#)]
10. Kate, K.; Wood, R.K.L. *Digital Imaging of Artefacts: Developments in Methods and Aims*; Archaeopress Publishing Ltd.: Oxford, UK, 2018.
11. Campanella, L.; Cardelicchio, F.; Dell'Aglio, E.; Reale, R.; Salvi, A.M. A green approach to clean iron stains from marble surfaces. *Herit. Sci.* **2022**, *10*, 79. [[CrossRef](#)]
12. Marvasi, M.; Donnarumma, F.; Frandi, A.; Mastromei, G.; Sterflinger, K.; Tiano, P.; Perito, B. Black microcolonial fungi as deteriorogens of two famous marble statues in Florence, Italy. *Int. Biodeterior. Biodegrad.* **2012**, *68*, 36–44. [[CrossRef](#)]
13. Santo, A.P.; Cuzman, O.A.; Petrocchi, D.; Pinna, D.; Salvatici, T.; Perito, B. Black on white: Microbial growth darkens the external marble of Florence cathedral. *Appl. Sci.* **2021**, *11*, 6163. [[CrossRef](#)]
14. Cuzman, O.A.; Vettori, S.; Fratini, F.; Cantisani, E.; Ciattini, S.; Chelazzi, L.; Ricci, M.; Garzonio, C.A. Alteration of marble stones by red discoloration phenomena. In *Science and Art: A Future for Stone: Proceedings of the 13th International Congress on the Deterioration and Conservation of Stone, Paisley, UK, 6–10 September 2016*; University of the West of Scotland: Glasgow, UK, 2016; p. 75.

15. Pinzari, F.; Zotti, M.; De Mico, A.; Calvini, P. Biodegradation of inorganic components in paper documents: Formation of calcium oxalate crystals as a consequence of *Aspergillus terreus* Thom growth. *Int. Biodeterior. Biodegrad.* **2010**, *64*, 499–505. [CrossRef]
16. Pinna, D.; Bracci, S.; Magrini, D.; Salvadori, B.; Andreotti, A.; Colombini, M.P. Deterioration and discoloration of historical protective treatments on marble. *Environ. Sci. Pollut. Res.* **2022**, *29*, 20694–20710. [CrossRef] [PubMed]
17. Gherardi, F.; Kapridaki, C.; Roveri, M.; Gulotta, D.; Maravelaki, P.N.; Toniolo, L. The deterioration of Apuan white marble in contemporary architectural context. *J. Cult. Herit.* **2019**, *35*, 297–306. [CrossRef]
18. Maxwell, I. Stone Cleaning: For Better or Worse? An Overview. In *Stone Cleaning and the Nature, Soiling and Decay Mechanisms of Stone, Proceedings of the International Conference, Edinburgh, UK, 14–16 April 1992*; Routledge: London, UK, 1992; pp. 3–49.
19. Fassina, V. General Criteria for the Cleaning of Stone: Theoretical Aspects and Methodology of Application. In *Stone Material in Monuments: Diagnosis and Conservation, Proceedings of the Scuola Universitaria CUM Conservazione dei Monumenti, Heraklion, Greek, 24–30 May 1993*; pp. 131–138. Available online: https://www.researchgate.net/profile/Vasco-Fassina-2/publication/345726155_GENERAL_CRITERIA_FOR_THE_CLEANING_OF_STONE_THEORETICAL_ASPECTS_AND_METHODODOLOGY_OF_APPLICATION_by_Vasco_Fassina/links/5fabde92299bf18c5b64de40/GENERAL-CRITERIA-FOR-THE-CLEANING-OF-STONE-THEORETICAL-ASPECTS-AND-METHODOLOGY-OF-APPLICATION-by-Vasco-Fassina.pdf (accessed on 20 August 2022).
20. Natali, I.; Carretti, E.; Angelova, L.; Baglioni, P.; Weiss, R.G.; Dei, L. Structural and mechanical properties of “peelable” organoaqueous dispersions with partially hydrolyzed poly (vinyl acetate)-borate networks: Applications to cleaning painted surfaces. *Langmuir* **2011**, *27*, 13226–13235. [CrossRef]
21. Zhenova, A. Challenges in the development of new green solvents for polymer dissolution. *Polym. Int.* **2020**, *69*, 895–901. [CrossRef]
22. Andreotti, A.; Colombini, M.P.; De Cruz, A. Er: YAG laser cleaning of a marble Roman urn. *J. Inst. Conserv.* **2020**, *43*, 12–24. [CrossRef]
23. Aldrovandi, A.; Lalli, C.; Lanterna, G.; Matteini, M. Laser cleaning: A study on greyish alteration induced on non-patinated marbles. *J. Cult. Herit.* **2000**, *1*, S55–S60. [CrossRef]
24. Ranalli, G.; Zanardini, E. Biocleaning on Cultural Heritage: New frontiers of microbial biotechnologies. *J. Appl. Microbiol.* **2021**, *131*, 583–603. [CrossRef]
25. Benocci, C. *Villa Ludovisi*; Istituto Poligrafico e Zecca dello Stato: Roma, Italy, 2010.
26. Broggi, L. *Le Residenze di s. M. La Regina Madre d’Italia, Margherita di Savoia*; Istituto d’Arti Grafiche: Bergamo, Italy, 1909; ISBN 1910 480.
27. Brunori, V. Art evening at palazzo Margherita. In *A Walk through the History and Art Collection of the Embassy of the United States of America in Rome*; Gangemi editore: Roma, Italy, 2006; ISBN 9788849210279.
28. Marchi, C. *Palazzo Margherita: The Embassy of the United States of America in Rome*; De Luca: Roma, Italy, 1980.
29. Schiavo, A. *Villa Ludovisi and Palazzo Margherita*; Roma amor per conto della Banca Nazionale del Lavoro: Roma, Italy, 1981.
30. Macchia, A.; Biribicchi, C.; Carnazza, P.; Montorsi, S.; Sangiorgi, N.; Demasi, G.; Prestileo, F.; Cerafogli, E.; Colasanti, I.A.; Aureli, H.; et al. Multi-Analytical Investigation of the Oil Painting “Il Venditore di Cerini” by Antonio Mancini and Definition of the Best Green Cleaning Treatment. *Sustainability* **2022**, *14*, 3972. [CrossRef]
31. Gervais, C.; Grissom, C.A.; Little, N.; Wachowiak, M.J. Cleaning marble with ammonium citrate. *Stud. Conserv.* **2010**, *55*, 164–176. [CrossRef]
32. Giraud, T.; Gomez, A.; Lemoine, S.; Pelé-Meziani, C.; Raimon, A.; Guilminot, E. Use of gels for the cleaning of archaeological metals. Case study of silver-plated copper alloy coins. *J. Cult. Herit.* **2021**, *52*, 73–83. [CrossRef]
33. Macchia, A.; Colasanti, I.A.; Rivaroli, L.; Favero, G.; de Caro, T.; Pantoja Munoz, L.; Campanella, L.; La Russa, M.F. Natural based products for cleaning copper and copper alloys artefacts. *Nat. Prod. Res.* **2021**. [CrossRef] [PubMed]
34. Delegou, E.T.; Avdelidis, N.P.; Karaviti, E.; Moropoulou, A. NDT&E techniques and SEM-EDS for the assessment of cleaning interventions on Pentelic marble surfaces. *X-ray Spectrom. Int. J.* **2008**, *37*, 435–443.
35. Toffolo, M.B.; Ricci, G.; Caneve, L.; Kaplan-Ashiri, I. Luminescence reveals variations in local structural order of calcium carbonate polymorphs formed by different mechanisms. *Sci. Rep.* **2019**, *9*, 16170. [CrossRef]
36. Vandenabeele, P.; Bodé, S.; Alonso, A.; Moens, L. Raman spectroscopic analysis of the Maya wall paintings in Ek’Balam, Mexico. *Spectrochim. Acta Part A Mol. Biomol. Spectrosc.* **2005**, *61*, 2349–2356. [CrossRef]
37. Bishop, J.L.; King, S.J.; Lane, M.D.; Brown, A.J.; Lafuente, B.; Hiroi, T.; Roberts, S.; Swayze, G.A.; Lin, J.-F.; Sánchez Román, M. Spectral properties of anhydrous carbonates and nitrates. *Earth Space Sci.* **2021**, *8*, e2021EA001844. [CrossRef]
38. Morbidelli, L. *Le Rocce e i Loro Costituenti. Scienze e Lettere*; Bardi Editore: Roma, Italy, 2003; ISBN 88-88620-20-6.
39. Gunasekaran, S.; Anbalagan, G.; Pandi, S. Raman and infrared spectra of carbonates of calcite structure. *J. Raman Spectrosc.* **2006**, *37*, 892–899. [CrossRef]
40. Monte, M. Oxalate film formation on marble specimens caused by fungus. *J. Cult. Herit.* **2003**, *4*, 255–258. [CrossRef]
41. Rampazzi, L.; Andreotti, A.; Bonaduce, I.; Colombini, M.P.; Colombo, C.; Toniolo, L. Analytical investigation of calcium oxalate films on marble monuments. *Talanta* **2004**, *63*, 967–977. [CrossRef] [PubMed]
42. Anastas, P.T.; Warner, J.C. Green chemistry. *Frontiers* **1998**, *640*, 1998.
43. Mahmoud, M.A.; Nasr-El-Din, H.A.; De Wolf, C.A.; Alex, A.K. Effect of Lithology on the Flow of Chelating Agents in Porous Media during Matrix Acid Treatments. In *Proceedings of the SPE Production and Operations Symposium, Oklahoma City, OK, USA, 13–23 March 2011*; OnePetro: Washington, DC, USA, 2011.

44. Adenuga, O.O.; Nasr-El-Din, H.A.; Sayed, M.A.I. Reactions of Simple Organic Acids and Chelating Agents with Dolomite. In Proceedings of the SPE Production and Operations Symposium, Oklahoma City, OK, USA, 23–26 March 2013; OnePetro: Washington, DC, USA, 2013.
45. Rabie, A.I. Reaction of Calcite and Dolomite with In-Situ Gelled Acids, Organic Acids, and Environmentally Friendly Chelating Agent (GLDA). Ph.D. Thesis, Texas A&M University, College Station, TX, USA, 2012.
46. Fredd, C.N.; Fogler, H.S. The influence of chelating agents on the kinetics of calcite dissolution. *J. Colloid Interface Sci.* **1998**, *204*, 187–197. [[CrossRef](#)] [[PubMed](#)]
47. Oviedo, C.; Rodríguez, J. EDTA: The chelating agent under environmental scrutiny. *Quim. Nova* **2003**, *26*, 901–905. [[CrossRef](#)]
48. Available online: <https://echa.europa.eu/it/substance-information/-/substanceinfo/100.112.462> (accessed on 20 August 2022).